

High quality $Y_3Al_5O_{12}$ doped transparent ceramics for laser applications, role of sintering additives

A A Kaminskii¹, V V Balashov², E A Cheshev^{3,4}, Yu L Kopylov², A L Koromyslov³, O N Krokhin^{3,4}, V B Kravchenko², K V Lopukhin², V V Shemet² and I M Tupitsyn⁴

¹ Shubnikov Crystallography Institute RAS, 59 Leninsky pr., 119333, Moscow, Russia

² Kotelnikov FIRE RAS, 1 Vvedensky Sq., 141120 Fryazino, Russia

³ P.N. Lebedev Physical Institute of the RAS, 53 Leninsky pr., 119991, Moscow, Russia

⁴ National Research Nuclear University MEPhI, 31 Kashirskoye shosse, 115409, Moscow, Russia

E-mail: ylk215@yandex.ru, additional ylk215@ire216.msk.su

Abstract. SiO_2 , ZrO_2 , B_2O_3 and MgO oxides and their combinations were used as sintering aids for preparation of yttrium aluminum garnet (YAG) ceramics doped by Nd_2O_3 , Er_2O_3 , Ho_2O_3 , Tm_2O_3 and Yb_2O_3 . The influence of these additives on optimal sintering temperature, grain growth, volume of residual pores and optical quality of the ceramics were investigated. The best combination of the sintering additives was found and high quality samples of YAG:Nd (1 at.%) ceramics were obtained. The original method of laser optical quality characterization of ceramics was developed and tested. The main laser parameters of YAG:Nd (1 at.%) ceramics samples are measured and compared with the best well known laser ceramics. The samples of YAG:RE (RE- Er_2O_3 , Ho_2O_3 , Tm_2O_3 and Yb_2O_3) ceramics are obtained, and their optical transmittance spectra are measured. Composite structures of YAG:Yb (5 at.%) – YAG were obtained by the simplest method of successive joint compaction of different composition layers.

1. Introduction

The main problem of doped YAG ceramics production technology with laser level of samples quality is elimination of residual pores. In the frames of solid state reactive sintering process a large number of factors effects on residual porosity such as appropriate morphology and dispersivity of starting oxide powders [1-4], stoichiometry of composition [5], conditions of compaction and sintering [6-10] and the presence of sintering additives (SA). There are attempts to produce ceramics without any (special) SA (see, for example, [11]). But practically all high quality ceramics were obtained with SA. As a rule, SA for oxide ceramics are different oxides. The most traditional SA for YAG is SiO_2 [12-15]. MgO and SiO_2 and MgO combinations were used in some very interesting and successful works [16-18]. There is no significant difference in results with SiO_2 and MgO , but in case of B_2O_3 and



combination of B_2O_3 and SiO_2 as SA there is a sharp contrast [19]. It was interesting to expand the research of application of the individual oxides and their possible combinations as sintering additives.

2. Experimental

High purity oxides Y_2O_3 , Nd_2O_3 , Er_2O_3 , Ho_2O_3 , Tm_2O_3 and Yb_2O_3 produced by Lanhit Ltd. and Al_2O_3 - AKP- 50 produced by Sumitomo Chem. Corp. and BMA 15 produced by Baikowski Corp. were used as starting powder materials for ceramics samples preparation. SiO_2 , ZrO_2 , B_2O_3 and MgO in different combinations were used as SA for $(Y_{1-x}RE_x)_3Al_5O_{12}$ (YAG:RE) compositions. The concentration ranges of SA were the following: B_2O_3 -(0.45 -1.5) mol.%; SiO_2 -(0.45-1.35) mol. %; MgO -(0.05-0.45) mol. %; ZrO_2 - 0.2 mol.%. All additives were reagent grade. Powders were weighed in ratios corresponding to the chemical composition and were mixed in planetary ball mill with anhydrous isopropanol and alumina balls. After milling and drying, the powders were sieved through 200 mesh sieve and mixed in the ball mill again with anhydrous isopropanol and PVB. After repeated drying and sieving the powders were pressed uniaxially at 50 MPa. PVB was evaporated at 800°C and compacts were finally pressed isostatically at 200-250 MPa. Compacts of YAG:RE compositions were vacuum sintered at 1500-1780°C. The heating rate was about 0,3°C/min at the temperatures around the maximum rate of shrinkage. Ceramics samples after sintering were annealed in air at 1100°C during 32 h. For crystallographic phase characterization the X-ray diffraction (XRD) machine D8 DISCOVER (Cu $K\alpha_{1,2}$ $\lambda = 1,542\text{\AA}$) was used. Shrinkage investigations during the sintering – thermomechanical analysis (TMA) were conducted with DIL402C, Netzsch and thermogravimetric and scanning calorimetric analysis (TGA, DSC) with NETZSCH STA 449 machines respectively. For pores contents measurement the light tomography method was used similar to the method described in [20]. The special setup was developed and used for lasing experiments. The description of this method is presented below.

3. Results and discussion

The temperature range of maximum rate of shrinkage during the sintering process for YAG: RE compositions depends strongly on the type and the combination of SA. The most remarkable combinations of SA investigated can be divided in to three groups: “1”- B_2O_3 (0.9)+ SiO_2 (0.9); “2”- B_2O_3 (1,5)+ SiO_2 (0.9)+ ZrO_2 (0.2); “3”- SiO_2 (1.35)+ MgO (x). The results of TMA investigation for these groups are shown in figure 1.

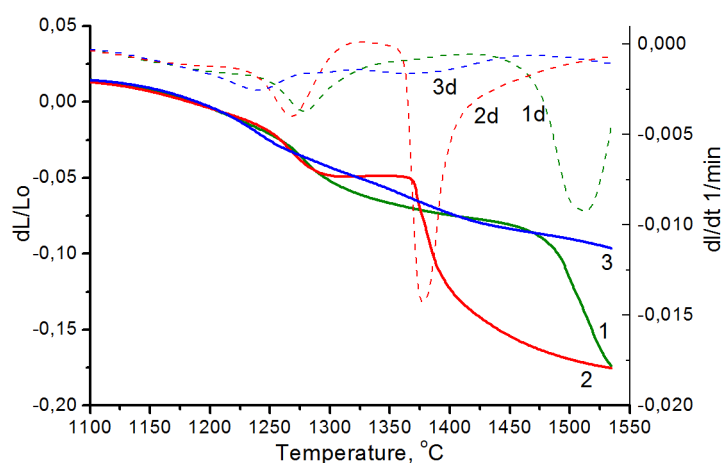


Figure 1. Temperature dependence of shrinkage (1,2,3) and rate of shrinkage (1d,2d,3d) for three groups of YAG: Nd (1at.%) ceramics.

Generally, the increase the SA concentration, especially B_2O_3 , shifts the maximum of shrinkage rate to lower temperatures. It was found, that it is possible to increase significantly B_2O_3 and SiO_2 contents without the deterioration of optical quality of the ceramic samples. At the same time the increase of ZrO_2 and MgO contents for more than 0.2 mol % results in increasing of residual porosity, and as a result the optical transmittance of ceramics drops down dramatically. XRD diagrams show that for B_2O_3 and/or SiO_2 contents above 0.6 mol % (that is for groups 1 and 2 in figure 1) the formation of garnet structure during the sintering was completed below $1550^\circ C$. In the contrast about 7 % of $Y_2Al_4O_9$ and $YAlO_3$ phases remained for group 3 at $1500^\circ C$ temperature, and the final formation of YAG phase was completed after $1550-1600^\circ C$. The difference of aluminate phases formation in groups 1 and 2 are demonstrated by general XRD diagrams presented in figure 2.

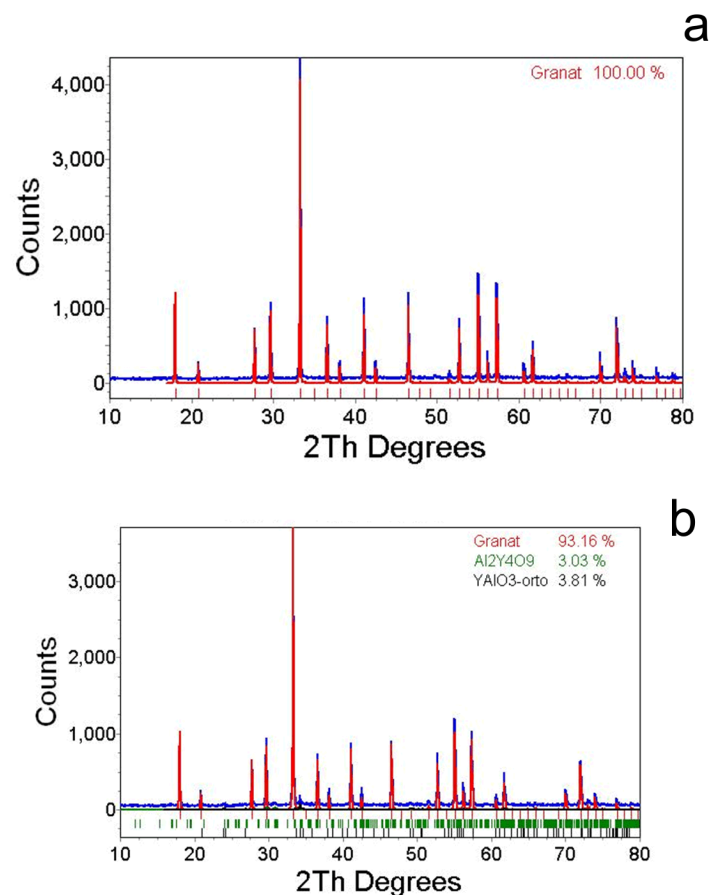


Figure 2. XRD diagrams of YAG samples sintered in dilatometer at $1550^\circ C$. Samples of 1 and 3 groups (a). samples of group1(b).

In shrinkage curves for all samples with content B_2O_3 there is a temperature range where shrinkage rate is near to zero. It is most pronounced for samples of group “2”. It can be explained by the reorientations of powder particles in presence of liquid phase created by SA. As was shown in [20-22] this reorientation range in presence of liquid phase comes really before shrinkage. The shift of maximum rate of shrinkage to lower temperatures increases the grain size and optical transmittance at every sintering temperature and decreases the residual porosity, as shown in figure 3 a, b and c.

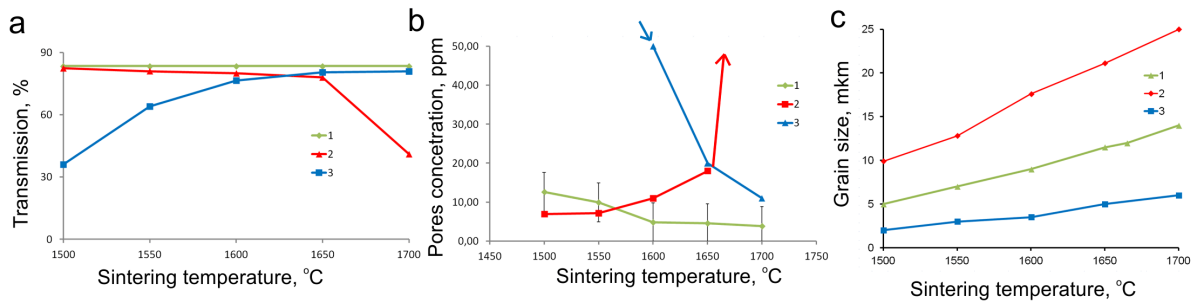


Figure 3. Characteristics of three groups (1,2,3) ceramic samples vs sintering temperature. a) Optical transmittance at $\lambda=1063$ nm. b) Residual pores concentration. c) Grain size.

The optical transmission reaches almost the theoretical level for group 1 before 1500°C and for group 3 before 1700°C. For group 2 transmittance drops down near 1700°C (see figure 3 a). These data are in reasonable correlation with concentration of the residual porosity (see figure 3 b). Unfortunately, at the same time the optical transmittance is growing together with increasing of grain size (compare the ratio between transmittance, porosity, figure 3 a, b) and grain size figure 3 c)). When a compromise between the grain size and optical transparency is found, it is possible to obtain the ceramics with high optical transparency for YAG: Nd (or Yb) samples with appropriate combination of SA. Examples of such ceramics and spectra of optical transmittance are presented in figure 4 for samples of YAG:Nd (1at.%).

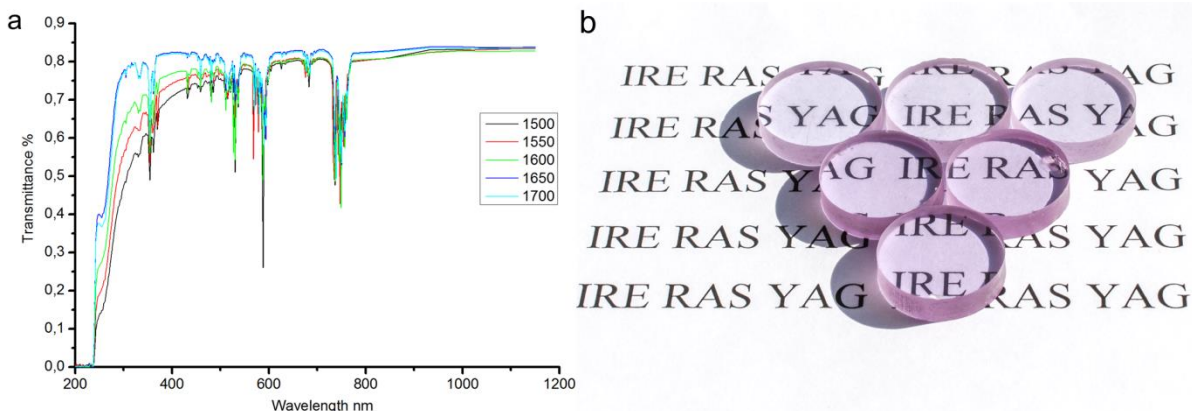


Figure 4. Optical inline transmittance of ceramics samples from group “2” (a) and general view of these ceramics (b). Insertion in a) is the sintering temperatures. Diameter of samples in b) is equal to 21 mm.

Dramatical decrease of transmittance and increase of the residual porosity for group 2 of samples at the sintering temperature can be explained probably by the presence of heterovalent zirconium cations.

The original method for measurement of lasing threshold at the longitudinal diode pumping nearly transverse mode locking was used for testing of lasing properties of the produced samples. The details of this method are described in detail elsewhere [23-25]. For the measurement procedure, the cavity length L of resonator is changed and power of the lasing threshold is automatically measured. The pumping of the sample is not uniform, and the transverse mode locking takes place at some values of length, L . Conditions of transverse mode locking can be determined by the following equation—condition of transverse mode locking for empty cavity [26]:

$$\arccos(\sqrt{g_1 g_2}) = \pi \frac{r}{s},$$

where r/s – proper fraction which characterize the degeneration [26], $g_{1,2} = 1 - L/R_{1,2}$ cavity stability parameter, L – cavity length, R – radius of mirrors.

At every L , near transverse mode locking, the pumping power value of lasing threshold decreases dramatically, and the value of threshold power at these conditions is very sensitive to any small optical heterogeneity of the laser media. Using the Konoshima Chemical corp. ceramic sample as etalon the spectra of pumping power value of lasing threshold were measured for four samples of our YAG: Nd (1at. %) ceramics with different concentration of residual pores. Results of these measurements are presented in figure 5.

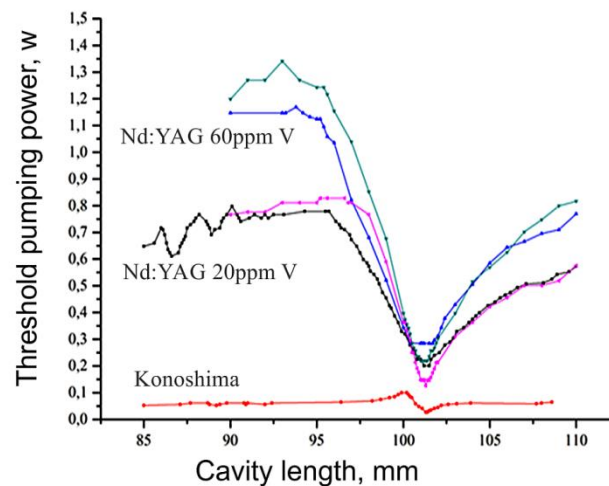


Figure 5. The pumping power corresponding to lasing threshold as a function of cavity length near the L value, where the proper fraction r/s is equal to $1/4$ for Konoshima ceramic YAG:Nd (1 at.%) sample and for two groups of ceramic YAG:Nd (1 at.%) samples with 20 and 60 ppm pores volume fractions.

The presented results show clearly that this method is really sensitive for defect detection in ceramic samples especially in the case of small concentration of residual pores. These data correspond to results obtained in work [27] by direct measuring output power of laser with ceramic samples which have different residual porosity. As it is seen in figure 5 the increasing of volume pores concentration from 1-2 ppm (for Konoshima ceramics) to 20 ppm and from 20 to 60 ppm increases the lasing threshold power by 10 and 20 times respectively. The comparative spectra for Konoshima's samples and our high quality samples like shown in figure 4 are presented in figure 6.

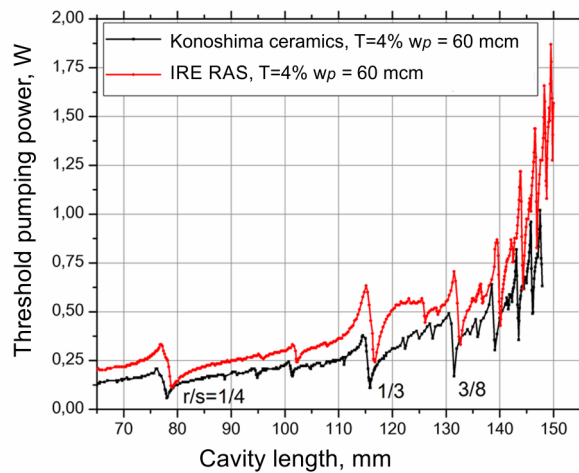


Figure 6. Pumping power corresponding to the lasing threshold as a function of cavity length for two YAG:Nd(1at. %) ceramic samples measured at the same conditions. w_p is radius of pumping beam, $T=4\%$ is reflectivity of output mirror.

Results for both types of samples are very close each to other. Some main laser characteristics were also measured for these high quality samples, and the results of these measurements are shown in figure 7. The data in figure 7 a) were obtained at the conditions when the pumping power was absorbed completely along the sample length. The slope efficiency determined from these measurements is 72 and 55 % for Konoshima samples and our ceramics respectively. The pulse duration is identical for both ceramics samples (see figure 7 b). The same quality ratio between the tested ceramic samples was found for such parameters as pulse power (figure 7 d), average output power (figure 7 e) and pulse duration (figure 7 c) as a function of output mirror reflectivity.

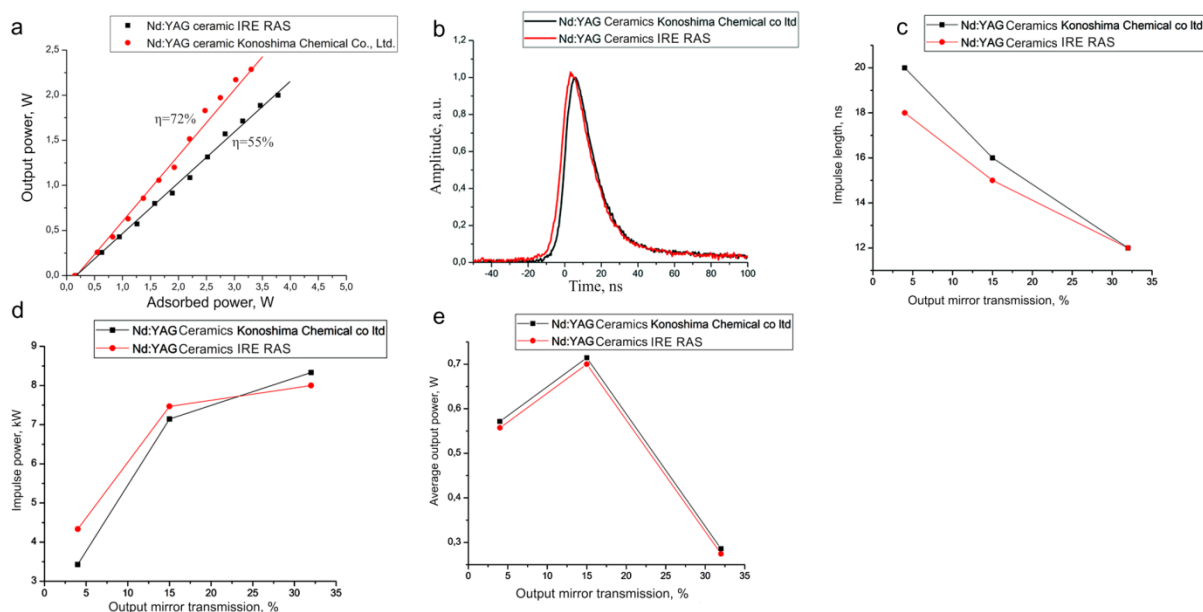


Figure 7. The main lasing characteristics of produced YAG:Nd(1at.%) ceramics in comparison with Konoshima etalon. Output power vs input power (a); impulse duration and shape (b), impulse length (c), impulse power (d) and average output power (e) as a function of output mirror transmission.

BMA-15 powder was used as Al_2O_3 source for manufacturing of samples YAG:RE, where RE=Yb₂O₃, Er₂O₃, Ho₂O₃, Tm₂O₃. Unfortunately, for samples of YAG with BMA-15 we did not achieve the same optical quality as in the case of AKP-50 powder. In these samples the residual pores in concentration about 20 ppm are existing. Probably it is due to not optimal milling condition for this powder. In figure 8 a, b the optical transmittance spectra and general view of $(\text{Y}_{2,91} \text{Tm}_{0,09})\text{Al}_5\text{O}_{12}$; $(\text{Y}_{2,85} \text{Yb}_{0,15})\text{Al}_5\text{O}_{12}$; $(\text{Y}_{2,985} \text{Ho}_{0,015})\text{Al}_5\text{O}_{12}$; $(\text{Y}_{2,985} \text{Er}_{0,015})\text{Al}_5\text{O}_{12}$ ceramics samples are presented.

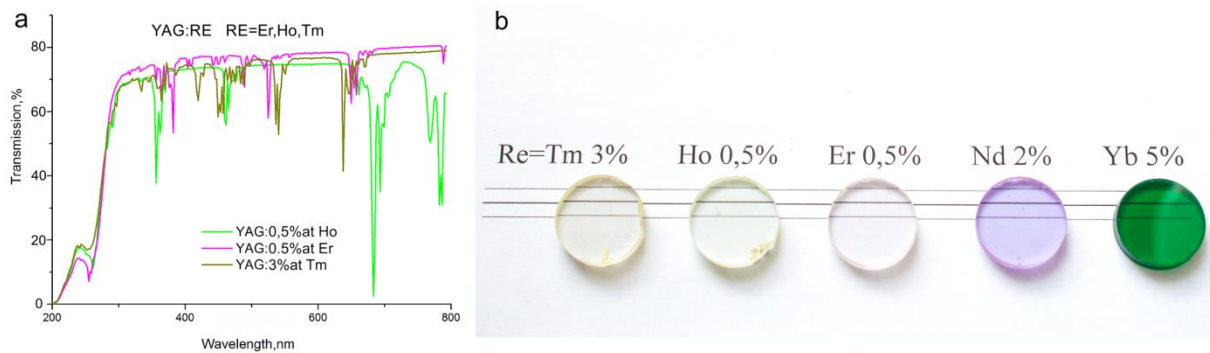


Figure 8. Optical in-line transmittance of $(\text{Y}_{2,91} \text{Tm}_{0,09})\text{Al}_5\text{O}_{12}$; $(\text{Y}_{2,85} \text{Yb}_{0,15})\text{Al}_5\text{O}_{12}$; $(\text{Y}_{2,985} \text{Ho}_{0,015})\text{Al}_5\text{O}_{12}$; $(\text{Y}_{2,985} \text{Er}_{0,015})\text{Al}_5\text{O}_{12}$ ceramics samples (a) and general view of the samples (b). Diameter of all samples in the photo is 21mm.

For YAG doped by Yb^{3+} the most attractive design of laser active elements is disk type. In this case, because the disc is thin enough, the composite structure with thick passive part is most profitable. Composite element must combine in monolithic ceramic body active (doped) and not active (not doped) parts. The simple method was used for preparation of the composite. In the metallic die the layer of YAG powder doped with Yb was pressed at 15-20 MPa, then the die was filled by non-doped YAG powder and pressed again at 50 MPa. The preformed compact was CIPed at 230 MPa and sintered by the method described early. The general view of the produced composite is shown in figure 9 a and b. After vacuum sintering Yb in YAG is in Yb^{2+} valence and has a green color. It is very comfortable for measurements of Yb^{2+} ions distribution by probe laser beam (λ -630 nm) scanning.

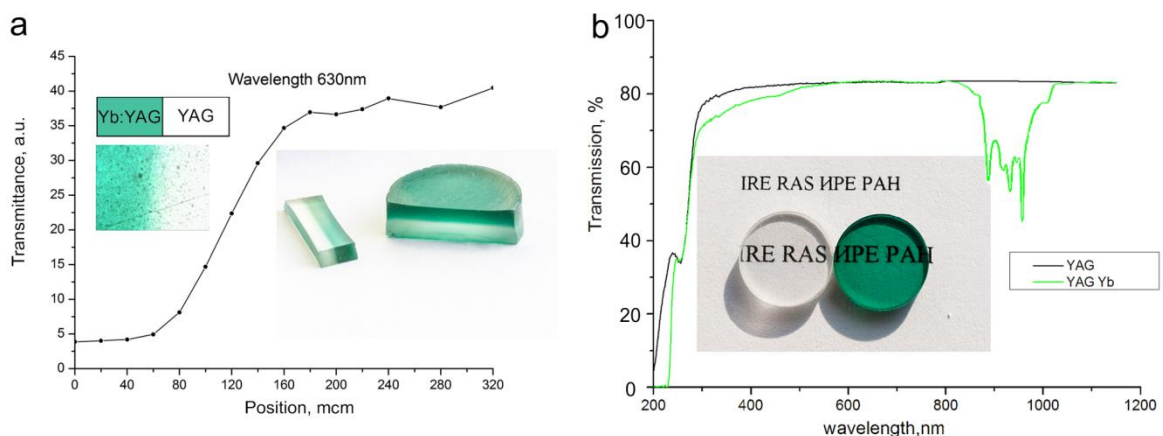


Figure 9. YAG:Yb(5 at.%) / YAG composite ceramics. In both photos in inserts (a, b) ceramic samples are as vacuum sintered and therefore Yb is as Yb^{2+} , that is green color. Distribution of Yb^{2+} near the border of two parts of the composite (a) which is measured as transmittance of light at λ -630 nm. Optical transmittance of doped and un-doped parts of the composite (b).

The results of these scanning measurements are shown in figure 9 b. It was found from these measurements that the width of transient region between two parts of the composite is about a hundred microns. It is a big value, and probably it can be explained by availability of intergrain fast diffusion. The optical transmission spectra of doped and undoped parts of YAG:Yb (5 at.%) - YAG composite are presented.

4. Conclusions

The role of sintering additives chosen from the group of SiO₂, ZrO₂, B₂O₃ and Mg in high quality YAG ceramics production was investigated. When contents of SiO₂ and especially B₂O₃ is growing up the grain size is increased, but the residual porosity decreased and the sintering temperature at which the optical transmittance achieves the theoretical values also decreased. The compromise between the grain size and residual porosity (optical transmittance) was found. The original method for estimation of ceramics optical quality was developed and tested on ceramics samples. Some of the main laser characteristics of produced ceramics YAG:Nd(1 at.%) were measured and compared with the best-known laser ceramics. The quality of the produced ceramics is comparable with the etalon. Composite structures of YAG:Yb (5 at.%) – YAG were obtained, and it was shown that consistent compaction of layers of different composition can be used as simple method for composite structures formation.

Acknowledgment

This work was performed in National Research Nuclear University MEPhI and in P.N. Lebedev Physical Institute of the Russian Academy of Sciences under the Agreement № 14.575.21.0047 with Ministry of Education and Science of Russian Federation, the unique identification number of applied scientific research RFMEFI57514X0047.

The authors acknowledge the generous financial support from Program of Presidium of Russian Academy of Sciences № P25, and Russian Foundation for Basic Research, project № 14- 02- 90446 Ukr_a.

This work was supported by the Competitiveness Program of National Research Nuclear University MEPhI.

References

- [1] Esposito L, Costa A L and Medri V 2008 Reactive sintering of YAG-based materials using micrometer-sized powders *J. Europ. Ceram. Soc.* **28** 1065-71
- [2] Ikesue A, Furusato I and Kamata K 1995 Fabrication of polycrystalline, transparent YAG ceramics by a solid-state reaction method *J. Am. Ceram. Soc.* **78**(1) 225
- [3] Liu Jun *et al* 2014 Effects of ball milling time on microstructure evolution and optical transparency of Nd:YAG ceramics *Ceram. Int.* **40** 7(A) 1271-8
- [4] Li Xiaodong, Li Ji-Guang, Xiu Zhimeng, Huo Di and Sun Xudong 2009 Transparent Nd:YAG Ceramics Fabricated Using Nanosized γ -Alumina and Ytria Powders *J. Am. Ceram. Soc.* **92** (1) 241–4
- [5] Patel A P, Levy M R, Grimes R W, Gaume R M, Feigelson R S, McClellan K J and Stanek C R 2008 Mechanism of nonstoichiometry in Y₃Al₅O₁₂ *Appl. Phys. Lett.* **93** 191902
- [6] Boulesteix R, Maitre A, Chretien L, Rabinovitch Y and Salle C 2013 Microstructural evolution during vacuum sintering of yttrium aluminum garnet transparent ceramics: toward the origin of residual porosity affecting the transparency *J. Am. Ceram. Soc.* **96** 1724-31
- [7] Kopylov Yu L, Kravchenko V B, Bagayev S N, Shemet V V, Komarov A A, Karban O F and Kaminskii A A 2009 Development of Nd³⁺:Y₃Al₅O₁₂ Laser Ceramics by High-Pressure Colloidal Slip-Casting (HPCSC) Method *Opt. Mater.* **31** (5) 707-10
- [8] Lin Ge, Jiang Li, Zhiwei Zhou, Binglong Liu, Tengfei Xie, Jing Liu, Huamin Kou, Yun Shi, Pan Yubai and Jingkun Guo 2015 Nd:YAG transparent ceramics fabricated by direct cold isostatic pressing and vacuum sintering *Opt. Mater.* **50** Part A December pp 25–31

- [9] Kwadwo A A, Messing G L and Dummc J Q 2008 Aqueous slip casting of transparent yttrium aluminum garnet (YAG) ceramics *Ceram. Int.* **34**(5) pp 1309-13
- [10] Wei Zhang, Lu Tiecheng, Maa B, Wei Nian, Lu Zhongwen, Li Feng, Guan Yongbing, Chen Xingtao, Liu Wei and Qi Lu 2013 Improvement of optical properties of Nd:YAG transparent ceramics by post-annealing and post hot isostatic pressing *Opt. Mater.* **35** 2405-10
- [11] Wang Z, Zhang Le, Yang H, Zhang J, Wang L, Zhang Q 2016 High optical quality Y_2O_3 transparent ceramics with fine grain size fabricated by low temperature air pre-sintering and post-HIP treatment *Ceram. Int.* **42** 4238-45
- [12] Ge L, Li Jiang, Zhou Zhiwei, Liu Binglong, Xie Tengfei, Liu Jing, Kou Huamin, Shi Yun, Pan Yubai and Guo Jingkun 2011 Effect of SiO_2 on Densification and Microstructure Development in Nd:YAG Transparent Ceramics *J. Am. Ceram. Soc.* **94** (5) 1380-7
- [13] Yagi H, Yanagitani T and Ueda K-I 2006 $Nd^{3+}:Y_3Al_5O_{12}$ laser ceramics: Flashlamp pumped laser operation with a UV cut filter. *J. Alloys Compd.* 421(1-2) 195
- [14] Yagi H, Yanagitani T, Takaichi K, Ueda K I and Kaminskii A A 2007 Characterizations and laser performances of highly transparent $Nd^{3+}:Y_3Al_5O_{12}$ laser ceramics *Opt. Mater.* **29** 1258-62
- [15] Gaume R, Markosyan He A and Baer R L 2012 Effect of Si-induced defects on 1 μm absorption in laser-grade YAG ceramics *J. Appl. Phys.* **111** 093104
- [16] Li Y K *et al* 2010 Fabrication of Nd:YAG transparent ceramics with TEOS, MgO and compound additives as sintering aids *J. Alloy. Compd.* **502**(1) 225e30
- [17] Yang H *et al* 2012 The effect of MgO and SiO_2 codoping on the properties of Nd:YAG transparent ceramic *Opt. Mater.* **34**(6) 940e3
- [18] Chen J C *et al* 2014 4350W quasi-continuous-wave operation of a diode face-pumped ceramic Nd:YAG slab laser *Opt. Laser. Technol.* **63** 50-3
- [19] Stevenson A J, Li X, Martinez M A, Anderson J, Suchy D L, Kupp E R, Dickey E C, Mueller K T and Messing G L 2011 Low temperature, transient liquid phase sintering of B_2O_3 - SiO_2 -doped Nd:YAG transparent ceramics *J. Mater. Res.* **26** 2022
- [20] Oh-Hun and Messsing G L 1991 A theoretical analysis of solution-precipitation controlled densification during piqued phase sintering *Acta Metall, Mater.* **39**(9) 2059-68
- [21] Kingery W D 1959 Densification during sintering in the presence of a liquid phase. I. Theory *J. Appl. Phys.* **30** 301-6
- [22] Kingery W D and Narasimham M D 1959 Densification during sintering in the presence of a liquid phase. II. Experimental *J. Appl. Phys.* **30** 307-10
- [23] Bezotosnyi V V, Cheshev E A, Gorbunkov M V, Koromyslov A L, Kostryukov P V, Krivonos M S, Popov Y M, Tunkin V G Behavior of threshold pump power of diode end-pumped solid-state lasers in critical cavity configurations 2015 *Laser Phys. Lett.* **12** (2) 025001
- [24] Bezotosnyi V V, Krokhin O N, Koromyslov A L Cheshev E A, Kopylov Y L, Kravchenko V B, Lopukhin K V, Tupizin I M 2015 Generation characteristics of YAG:Nd laser with YAG: Cr^{4+} passive lock on the base of oxide ceramics *Proceedings of V symposium on coherent optical radiation of semiconductor compounds and structures. Moscow-Zvenigorod 23-26 November* (Moscow, Lebedev Physical Institute RAS) (in Russian)
- [25] Kaminskii A A, Balashov V V, Demianova L, Kopylov Y L, Kravchenko V B, Lopukhin K V, Lyapin A A, Lysenko S L, Ryabochkina P A and Shemet V V 2015 Transparent Y_2O_3 and $Y_3Al_5O_{12}$ Ceramics Doped by Rare Earth Cations - Technology, Optical Properties, Problems and Prospects *Proceedings of 11-th laser ceramics symposium LCS-2015 – International symposium on transparent ceramics for photonics applications, 30 Nov.- 4 Dec. Xuzhou, China* pp 63-4
- [26] Wu H H, Sheu C C, Chen T W, Wei M D and Hsieh W F 1999 *Opt. Commun.* **165** 225-9
- [27] Boulesteix R, Maître A, Baumard J-F, Rabinovitch Y and Reynaud F 2010 Light scattering by pores in transparent Nd:YAG ceramics for lasers: correlations between microstructure and optical properties *Opt. Express* **18** (14) 14992